JCTC Journal of Chemical Theory and Computation

Article

pubs.acs.org/JCTC

Efficient Algorithms for Langevin and DPD Dynamics

N. Goga, A. J. Rzepiela, A. H. de Vries, S. J. Marrink, and H. J. C. Berendsen*

Groningen Biomolecular Sciences and Biotechnology Institute, Zernike Institute for Advanced Materials, University of Groningen, Nijenborgh 7, 9747 AG Groningen, The Netherlands

ABSTRACT: In this article, we present several algorithms for stochastic dynamics, including Langevin dynamics and different variants of Dissipative Particle Dynamics (DPD), applicable to systems with or without constraints. The algorithms are based on the impulsive application of friction and noise, thus avoiding the computational complexity of algorithms that apply continuous friction and noise. Simulation results on thermostat strength and diffusion properties for ideal gas, coarse-grained (MARTINI) water, and constrained atomic (SPC/E) water systems are discussed. We show that the measured thermal relaxation rates agree well with theoretical predictions. The influence of various parameters on the diffusion coefficient is discussed.

1. INTRODUCTION

The purpose of this article is to present simple and efficient algorithms for stochastic dynamics, in particular for simple Langevin dynamics and for various variants of the pairwise DPD (Dissipative Particle Dynamics) thermostat. The latter are Galilean invariant; i.e., the motion is the same in a coordinate system that moves with constant velocity, which is equivalent to the conservation of total linear momentum. In contrast, the simple Langevin dynamics will damp all velocities, including a bulk flow component. Galilean invariance is essential for simulations that are required to follow Navier−Stokes behavior in the macroscopic limit but is irrelevant for systems at rest. We require of such algorithms that they have the same order of accuracy as the Verlet (or leap-frog or velocity-Verlet) algorithms that are used in the frictionless case; in the limit of small friction, they should be equivalent to these algorithms. They should be valid for any value of the friction constant, not only in the limit of small friction. They should maintain the canonical distribution and act as a proper thermostat: i.e., the temperature derived from the average kinetic energy should converge to the reference temperature used in the algorithm.

The design of stochastic algorithms for molecular simulation was an important subject of research in the 1980s for van Gunsteren et al.[1−4] Van Gunsteren and Berendsen's 1988 paper[4] describes a sophisticated algorithm that fully maintains the accuracy of the Verlet algorithm by integrating the stochastic term over the time step. This algorithm is still standard in both the GROMOS and Gromacs simulation packages.

Stochastic thermostats have an advantage over the usual global thermostats that they maintain the correct canonical distribution and show a robust first-order decay of temperature deviations toward the reference temperature. Global thermostats of the *weak-coupling* type[5] show a convenient first-order decay of temperature deviations but do not maintain a canonical distribution; in fact, the resulting distribution is in between a canonical and a microcanonical distribution, depending on the coupling constant used.[6] Moreover, it is known that such thermostats may cause an uneven distribution of kinetic energy among different collective degrees of freedom, resulting in overheating of collective degrees of freedom that are only weakly coupled to the other degrees of freedom at the expense of cooling of these other degrees of freedom (the *flying ice-cube effect*[7]). The *velocity rescaling thermostat* of Bussi et al.[8] is a global weak-coupling thermostat in which the velocities are scaled such that the temperature follows a stochastic first-order process that ensures a canonical distribution for the global temperature. This solves the problem of an unknown ensemble, but it is not known if it also solves the flying ice-cube effect. Global thermostats of the *extended-system* type, such as the Nosé-Hoover thermostat,[9] will maintain a canonical distribution in configurational space but show strong oscillatory behavior of the temperature deviation as a result of the order of the differential equation related to the system's extension. The Nosé-Hoover *chain* thermostat,[10] using a cascade of thermostats, alleviates but does not solve this problem. See Berendsen,[11] pp 194−204, for a comparative discussion of thermostats.

The simple Langevin equations of motion[11] (i.e., Markovian and no frictional coupling between degrees of freedom) are for the ith degree of freedom in a Cartesian system of coordinates:

$$\dot{x}_i(t) = v_i(t) \tag{1}$$

$$\dot{v}_i(t) = a_i(t) - \gamma_i v_i(t) + \eta_i(t) \tag{2}$$

where $a_i(t)$ is the acceleration of the ith degree of freedom:

$$a_i(t) = \frac{F_i(\{\mathbf{r}(t)\})}{m_i} \tag{3}$$

and $\eta_i(t)$ is a random process with zero mean, no correlation with any past or present x or v, and with an autocorrelation function

$$\langle \eta_i(t)\eta_j(t+\tau)\rangle = 2\frac{k_B T_{ref}}{m_i}\gamma_i \delta(\tau)\delta_{ij} \tag{4}$$

Here, γ_i is the *friction rate* applied to the ith degree of freedom. [We reserve the name "friction constant" for the proportionality

Special Issue: Wilfred F. van Gunsteren Festschrift

Received: February 1, 2012
Published: June 13, 2012

constant between friction force and velocity, which equals the mass of the particle times the friction rate.]

This equation—and its DPD equivalent,[12−14] which applies friction and noise to *velocity differences* between particle pairs—is a stochastic differential equation. We note that eq 2 is a formal equation that is mathematically incorrect because $v(t)$ is not differentiable; it should be implemented as a difference equation over a small time step h:

$$\Delta v_i = a_i(t)h - \gamma_i v_i(t)h + \sqrt{2k_B T_{ref}\gamma_i h/m_i}\,\xi \tag{5}$$

for small h, where ξ is a normally distributed random number with unit variance. The last term is obtained by integrating the noise term in eq 2 over the time step h.

It can be shown that the velocity distribution will converge to a Maxwellian distribution at the reference temperature T_{ref}. The correct behavior as a thermostat is implicit in the equations and will be guaranteed only if the equations are solved exactly.

Algorithms to solve such equations in finite time steps are only exact in the limit of small h because of the position-dependent force; however, the stochastic terms can be integrated exactly over any time step. Algorithms[2,4,15] that integrate the stochastic equations of motion over a time step become very complex, requiring the sampling of two random variables from a bivariate distribution.

The same applies to most algorithms used for DPD. While for Langevin dynamics integration over the frictional and stochastic terms can be carried out over a time step, for the pairwise DPD friction and noise, this is not possible. Thus, for DPD, an additional complicating factor arises: friction and noise that are needed to update the velocity depend on the velocity itself. Accurate algorithms require iterative solutions for the velocity update. Various algorithms based on the velocity-Verlet scheme have been compared by Nikunen et al.[16]

A different approach, pioneered by Peters[17] for the case of DPD, leads to simpler and still correct algorithms. The principle is to consider the physical process as a sequence of a Hamiltonian evolution over one time step, followed by an *impulsive* action of friction and noise. The latter modifies the velocities without advancing the time. Thus, the evolution in phase space is the approximate application of the Liouville operator over a time step, followed by a transformation defined by the impulsive friction and noise. If it can be proven that this impulsive action also leads to convergence to a canonical (i.e., Maxwellian) distribution at the reference temperature, this physical process is equally valid to achieve our goal of introducing an effective thermostat. The energy and momentum transfer implicit in the impulsive friction will influence transport properties in a controllable way. The behavior as a thermostat will be robust, while the algorithm remains very straightforward and simple to implement. The principal difference with the usual stochastic differential equation is that the time evolution of the system is not described by a single stochastic differential equation but by a sequential application of a Hamiltonian evolution over a time step and an impulsive stochastic action on the velocities. Both steps should conserve the canonical distribution in phase space.

This approach is reminiscent of the principle of the Andersen thermostat,[18] which applies impulsive redistributions to particle velocities with a probability Γh from a Maxwellian distribution. The same thermostatting method was introduced for DPD by Lowe.[19] The Andersen and Lowe thermostats do not reduce velocities with an adjustable friction but reduce the velocity completely to zero, followed by a noise term equal to a sampling from the full Maxwellian distribution. The impulsive change introduced this way is locally (in time and space) quite large and disrupts the smooth evolution of the trajectory. The impulsive friction and noise as applied by Peters spreads the changes much more smoothly over time and space by applying small impulsive changes to every particle at every step.

In the following, we extend Peters' DPD-type impulsive friction and noise (which applies relative velocity changes in the interparticle direction only) to more general types. These include the traditional Langevin dynamics, which does not conserve linear momentum, and pairwise Galilean-invariant friction and noise acting on velocity differences. The latter can be applied to all three velocity components, or restricted to components either parallel or perpendicular to the interparticle direction. For each case, we investigate the effective thermostat strength implied by the impulsive application of friction and noise. We also investigate whether the pairwise application can be made more efficient by restricting friction and noise to one or a few neighbors, rather than all neighbors within a given range. For the ideal gas, we derive the diffusion coefficient, imposed by friction and noise. While Peters implements friction and noise in the velocity-Verlet integration scheme, we employ the popular leap-frog integration scheme. In all cases, we consider the implementation when the system contains holonomic constraints, and we consider the consequences for the computation of pressure.

This article is organized in the following way. In the following two sections, the impulsive scheme is discussed for Langevin dynamics using the leap-frog algorithm, for systems without constraints (section 2) and with constraints (section 3). Section 4 presents its application to pairwise interactions. In section 5, an *effective* average friction rate is defined that serves as a comparable friction rate measure, with a comparable influence on diffusion, for any type of impulsive friction imposed on the system. Section 6 describes the simulation details and reports the computational efficiency of the different methods; section 7 gives the results of various tests of the algorithms on different molecular systems (ideal gas, coarse-grained water without constraints, and atomic water with constraints). Both thermostat and diffusion behavior are considered. Section 8 discusses the results and summarizes the conclusions.

2. THE IMPULSIVE LANGEVIN LEAP-FROG ALGORITHM FOR SYSTEMS WITHOUT CONSTRAINTS

Consider a system of n particles with $3n$ degrees of freedom, and consider every degree of freedom separately. Assume $v(t - (1/2)h)$, $x(t)$, and $F(t) = ma$ are the known velocity, coordinate, and force components, and a is the acceleration at time t of that degree of freedom. The impulsive Langevin extension of the leap-frog algorithm then reads as follows:

For all degrees of freedom, do:

1. $v = v\left(t - \frac{1}{2}h\right) + ah$

2. $\Delta v = -fv + \sqrt{f(2-f)(k_B T_{ref}/m)}\,\xi$

3. $x(t + h) = x(t) + \left(v + \frac{1}{2}\Delta v\right)h$

$$4.\ v\left(t+\frac{1}{2}h\right) = v + \Delta v$$

Here, step 1 is the usual MD velocity-update of the leap-frog scheme; step 2 is the impulsive application of friction (reducing the velocity by a fraction f: $0 \le f \le 1$) and noise (ξ is a random sample from a normal distribution). Step 3 updates the coordinates, taking into account that Δv is applied only between $t + (1/2)h$ and $t + h$: in fact, step 3 can be considered as two half steps (see Figure 1):

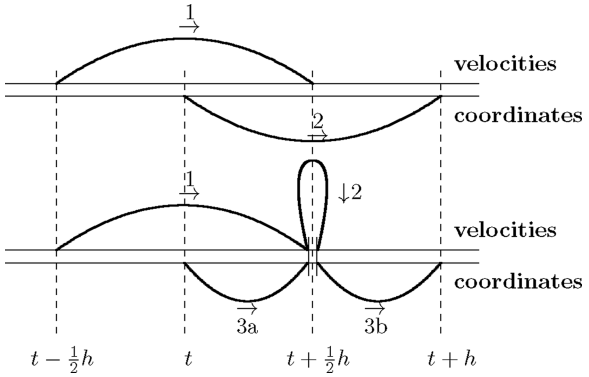

Figure 1. (Top) Traditional leap-frog scheme. (Bottom) Leap-frog scheme with impulsive phase.

$$3a.\ x\left(t+\frac{1}{2}h\right) = x(t) + v\frac{1}{2}h$$

$$3b.\ x(t+h) = x\left(t+\frac{1}{2}h\right) + (v+\Delta v)\frac{1}{2}h$$

Step 4 assigns the modified velocity to the velocity at the end of the time step. It is irrelevant whether these steps are carried out sequentially per degree of freedom, sequentially per 3-D vector per particle, or each performed on a $3n$-D vector over all degrees of freedom.

The variance of the noise term is chosen such that the variance of the velocity

$$\langle (v+\Delta v)^2 \rangle = (1-f)^2 \langle v^2 \rangle + f(2-f)\frac{k_B T_{ref}}{m} \tag{6}$$

tends to the stationary value of $k_B T_{ref}/m$. This is easily seen from eq 6 by substituting $k_B T_{ref}/m$ for each of the mean squared velocities.

In this algorithm, it is assumed that all degrees of freedom are subjected to the same friction and noise at every time step; this is just a convenient scheme that could be replaced by other variants, e.g., different f's for different particles, or application of friction and noise to a (randomly) selected subset at every step. Note that the limiting case $f = 1$ completely removes the velocity and replaces it by a sample from a Maxwellian distribution. Thus, if the impulsive friction and noise is applied with $f = 1$ and with a probability Γh per particle per step, the Andersen thermostat is recovered. A *smoothed Andersen thermostat* with the same *average* velocity reduction factor will be obtained by applying the impulsive friction and noise with $f = \Gamma h$ every step to every degree of freedom.

The algorithm is expected to be robust, in the sense that the impulsive term is exact, independent of the time step used. There is a lot of freedom of choice in the way the impulsive term is applied: the damping factor f may be applied to a random selection of particles and may differ for different particles. The application to velocity differences as in DPD is straightforward (see section 4).

It is obvious that the new velocity of any particle does not have the same direction and magnitude as its old velocity. As the random changes are uncorrelated, the total momentum is not conserved and neither is the total energy conserved. However, the average kinetic energy and hence the temperature will be stable: they tend toward the values determined by the reference temperature.

2.1. Is the Velocity Distribution Canonical? In order to judge the acceptability of the proposed procedure, we ask the following questions: *Assume the velocity distribution before the impulse is $\rho_0(v)$: (a) What will be the distribution $\rho_1(v + \Delta v)$ after the impulse? (b) What is the stationary distribution?*

After the impulse, the distribution $\rho_1(v + \Delta v)$ is the convolution of the original distribution $\rho_0(v)$ and the Gaussian distribution of the random term $\Delta v + fv$, which has a variance of $f(2 - f)k_B T_{ref}$:

$$\rho_1(w) = [2\pi f(2-f)k_B T_{ref}]^{-1/2} \int_{-\infty}^{\infty} dv\ \rho_0(v) \times \exp\left[-\frac{\{w-(1-f)v\}^2}{2f(2-f)k_B T_{ref}}\right] \tag{7}$$

where $w = v + \Delta v$. This is the answer to question a. The answer to question b is found by inserting the canonical distribution for v:

$$\rho_0(v) = [2\pi k_B T_{ref}]^{-1/2} \exp\left[-\frac{v^2}{2k_B T_{ref}}\right] \tag{8}$$

into eq 7. Carrying out the integration over v, we find that $\rho_1(w)$ is exactly equal to the same canonical distribution ρ_0. So, $\rho_0(v)$ is the stationary distribution. Thus, the impulsive application of friction and noise not only preserves the variance (as designed) but preserves the complete canonical distribution as well.

2.2. How Does the Temperature Behave with Time? A good thermostat should force a deviation from the reference temperature back to zero. How does the impulsive Langevin thermostat behave in this respect?

Consider one dimension. The temperature is given by

$$T = \frac{m}{k_B}\langle v^2 \rangle \tag{9}$$

The energy change ΔE_1 resulting from a single application of friction and noise to one degree of freedom is

$$\Delta E_1 = \frac{1}{2}m(v+\Delta v)^2 - \frac{1}{2}mv^2 \tag{10}$$

Using eqs 6 and 9, this rewrites to

$$\Delta E_1 = \frac{1}{2}f(2-f)\,k_B(T_{ref} - T) \tag{11}$$

the total energy change *per time step* h is the sum over all one-dimensional frictional events that occur per time step:

$$\Delta E_{tot} = \frac{1}{2}k_B \sum f(2-f)(T_{ref} - T) \tag{12}$$

The energy change is initially supplied to the kinetic energy of the system, thus changing the temperature. However, when the

dx.doi.org/10.1021/ct3000876 | J. Chem. Theory Comput. 2012, 8, 3637−3649

rate of change is small, the energy change will be distributed over kinetic and potential energy. The temperature change is then determined by the total heat capacity C_V of the system:

$$\Delta T = \frac{\Delta E_{\mathrm{tot}}}{C_V} \tag{13}$$

yielding a differential equation for the time dependence of the temperature:

$$\frac{dT}{dt} = \frac{1}{2}k_{\mathrm{B}}\frac{\sum f(2-f)}{C_V h}(T_{\mathrm{ref}} - T) \tag{14}$$

In the case of a three-dimensional application to N particles, eq 14 has the form

$$\frac{dT}{dt} = \frac{3k_{\mathrm{B}}}{2c_V}\frac{f(2-f)}{h}(T_{\mathrm{ref}} - T) \tag{15}$$

where

$$c_V = \frac{C_V}{N} \tag{16}$$

is the specific heat per particle.

Equation 15 shows that any deviation from the reference temperature will decay to zero according to a first-order kinetic process

$$\frac{dT}{dt} = k_{\mathrm{th}}(T_{\mathrm{ref}} - T) \tag{17}$$

with rate constant

$$k_{\mathrm{th}} = \frac{3k_{\mathrm{B}}}{2c_V}\frac{f(2-f)}{h} \tag{18}$$

Alternatively, the decay can be characterized by a time constant $\tau_T = 1/k_{\mathrm{th}}$. Note that for an ideal gas, $c_V = (3/2)k_{\mathrm{B}}$, reducing the left fraction in eq 18 to 1; for atomic fluids, this fraction is usually 2 to 3 times smaller.

The thermal rate constant can be expressed in an *effective friction rate* γ_{eff}, defined by the continuous friction rate that would reduce the velocity per time step h by a fraction f:

$$\gamma_{\mathrm{eff}} \stackrel{\mathrm{def}}{=} -\frac{1}{h}\ln(1-f) \tag{19}$$

yielding

$$k_{\mathrm{th}} = \frac{3k_{\mathrm{B}}}{2c_V}\frac{[1-\exp(-2\gamma_{\mathrm{eff}}h)]}{h} \approx \frac{3k_{\mathrm{B}}}{2c_V}2\gamma_{\mathrm{eff}} \tag{20}$$

the latter value being a good approximation for small γh.

Thus, the thermostat is robust: the system temperature automatically decays to the reference temperature, and the velocity distribution evolves into the proper canonical (Maxwellian) distribution.

Slow and Fast Thermostats. We note that this rate equation is valid when the rate constant of the thermostat is smaller than the rate of exchange between the kinetic and potential energy of the system, which gives the system time to equilibrate between kinetic and potential degrees of fzreedom. Usually, this condition is fulfilled. If, on the other hand, k_{th} is much larger ("fast" thermostats), C_V in eq 13 should be replaced by $E_{\mathrm{kin}}/T = (1/2)k_{\mathrm{B}}n_{\mathrm{dof}}$, where n_{dof} is the number of degrees of freedom in the system. The equivalent of eq 14 for fast thermostats is

$$\frac{dT}{dt} = \frac{\sum f(2-f)}{n_{\mathrm{dof}}h}(T_{\mathrm{ref}} - T) \tag{21}$$

where the sum is taken over all one-dimensional frictional events that occur per time step. This means that for a fast thermostat, c_V in eq 20 should be replaced by its ideal-gas value $3k_{\mathrm{B}}/2$.

3. IMPULSIVE LANGEVIN ALGORITHMS FOR SYSTEMS WITH CONSTRAINTS

Here, we give the algorithm for simple Langevin dynamics with constraints (section 3.3). For clarity, we first give the leap-frog algorithms for frictionless systems without constraints (section 3.1)—already mentioned in section 2—and with constraints (section 3.2).

3.1. No Constraints, No Friction. Consider a conservative system with n particles ($3n$ degrees of freedom). Assume $\mathbf{v}(t - (1/2)h)$ and $\mathbf{x}(t)$ are the known velocity and coordinate vectors (length $3n$) at the beginning of the time step. The leap-frog algorithm then advances one time step as follows ($i = 1, ..., 3n$):

1. Compute forces $\mathbf{F} = -\nabla V(\mathbf{x}(t))$ and compute virial using $\mathbf{x}(t)$.
2. Advance velocities $\forall i$: $v_i(t + (1/2)h) = v_i(t - (1/2)h) + (F_i/m_i)h$ (optional: adjust $\forall i$, $v_i(t + (1/2)h)$ according to global thermostat).
3. Advance positions $\forall i$: $x_i(t + h) = x_i(t) + v_i(t + (1/2)h)h$

3.2. Constraints, No Friction. Constraints are satisfied by calling a routine constr (SHAKE,[20] LINCS,[21] SETTLE[22]) that makes corrections to an unconstrained configuration $\mathbf{x}^{\mathrm{u}}$ to yield a configuration $\mathbf{x}^{\mathrm{c}}$ that satisfies the set of m holonomic constraints $\sigma_k(\mathbf{x}) = 0$, $k = 1, ..., m$. The displacements are in the direction of a reference configuration $\mathbf{x}^{\mathrm{ref}}$:

$$\mathbf{x}^{\mathrm{c}} = \mathrm{constr}(\mathbf{x}^{\mathrm{u}}; \mathbf{x}^{\mathrm{ref}}) \tag{22}$$

The routine constr also computes the constraint forces and evaluates the contribution to the virial (using the reference positions) due to the constraint forces. The algorithm of section 3.1 is now modified to:

1. Compute unconstrained forces $\mathbf{F}^{\mathrm{u}} = -\bigtriangledown V(\mathbf{x}(t))$ and compute virial using $\mathbf{x}(t)$.
2. Advance velocities $\forall i$: $v_i = v_i(t - (1/2)h) + (F_i^{\mathrm{u}}/m_i)h$ (optional: adjust $\forall i$, v_i according to global thermostat).
3. Advance positions $\forall i$: $x_i = x_i(t) + v_i h$.
4. Apply constraints to new positions: $\mathbf{x}(t + h) = \mathrm{constr}(\mathbf{x}; \mathbf{x}(t))$ and add constraint contribution to virial.
5. Reconstruct velocities $\forall i$: $v_i(t + 1/2) = [x_i(t + h) - x_i(t)]/h$.

Steps 4 and 5 ensure that the motion takes place on the hypersurface in configurational space, defined by the constraints. Any deviation from this hypersurface due to force components in the constraint directions (steps 2 and 3) is removed by the projection onto the constraint hypersurface in steps 4 and 5. We note that the reconstruction of velocities from coordinate differences introduces a noticeable, but avoidable, error when single-precision arithmetic is employed.[23]

3.3. Constraints Plus Impulsive Friction and Noise. We now modify the algorithm of section 2 to include an impulsive friction and noise:

1. Compute unconstrained forces $\mathbf{F}^{u} = -\nabla V(\mathbf{x}(t))$ and compute virial using $\mathbf{x}(t)$.
2. Advance velocities $\forall i$: $v_i = v_i(t - (1/2)h) + (F_i^{u}/m_i)h$.
3. Advance positions $\forall i$: $x_i = x_i(t) + v_i h$.
4. Apply constraints to new positions: $\mathbf{x}^{c} = \mathrm{constr}(\mathbf{x}; \mathbf{x}(t))$ and add constraint contribution to virial.
5. Reconstruct velocities $\forall i$: $v_i^{c} = [x_i^{c} - x_i(t)]/h$.
6. Apply friction and noise $\forall i$: $v'_i = (1 - f)v_i^{c} + (f(2 - f)(k_B T_{ref}/m_i))^{1/2}\xi_i$.
7. Correct positions for velocity change $\forall i$: $x'_i = x_i^{c} + (1/2)(v'_i - v_i^{c})h$.
8. Apply constraints to corrected positions: $\mathbf{x}(t + h) = \mathrm{constr}(\mathbf{x}'; \mathbf{x}(t))$. Do **not** add constraint contribution to virial.
9. Reconstruct velocities $\forall i$: $v_i(t + (1/2)h) = v_i^{c} + 2[x_i(t + h) - x'_i]/h$.

Note that the constraint algorithm is applied twice: the first time in step 4 to correct the effect of the unconstrained forces (this application also provides the conservative constraint force and computes the constraint contribution to the virial) and the second time in step 8 to annihilate the effects of friction and noise in the constraint directions. The latter concerns nonconservative forces acting on the velocities, which do not contribute to the virial. See Hess et al.[21] for details on how to compute the virial from constraint forces.

The impulsive friction and noise in step 6 is similar to step 2 in the unconstrained Langevin dynamics of section 2. The correctness of this procedure is not immediately clear because $\langle v_i^2 \rangle \neq k_B T/m_i$ when the particle is involved in constraints. However, the "excess" noise generated by step 6 is eliminated by the subsequent application of constraint corrections. This is strictly valid only in the limit of small friction (small f); for finite f, an error remains due to the fact that the application of friction and noise does not commute with the application of the constraint solver. In fact, for $f = 1$ (Andersen thermostat), a substantial error in the temperature may occur when the velocities of *selected* degrees of freedom are randomized in a system with constraints. Only when *all* degrees of freedom in a molecule with internal constraints are randomized will a canonical distribution at the reference temperature be obtained, as has been rigorously proven by Ryckaert and Ciccotti.[24] That an f-dependent error remains for a system with constraints is shown in Figure 3b (section 7.1).

4. PAIRWISE APPLICATIONS

The essence of DPD-like friction and noise is that it is applied to velocity *differences* (or relative velocities) between pairs of particles. If done properly, the pairwise application ensures conservation of linear momentum, both globally and locally over distances in the order of the particle interaction range. The friction and noise can be applied isotropically to the velocity difference vector, irrespective of its direction, but the velocity difference can also be split into a component parallel to the interparticle vector and a component perpendicular to it. The full vector is three-dimensional. The parallel component is one-dimensional, and the perpendicular component is defined in a plane and is therefore two-dimensional. In pure DPD,[14] only the parallel component is used. The perpendicular form has been introduced by Junghans et al.[25] The isotropic three-dimensional form is in fact a combination of both. Only the parallel component conserves angular momentum; however, the perpendicular component resembles more closely the viscous forces that cause shear viscosity. Which option is best depends on the purpose of the introduction of stochastic terms: for thermostatting, the parallel component is preferred; for mimicking viscous behavior, one may choose the isotropic or perpendicular case.

We shall consider all three possibilities. In each case, there is a damping rate γ and velocity reduction factor $f = 1 - \exp(-\gamma h)$ as in eq 19. These factors are dependent on the interparticle distance: a cutoff distance should be chosen beyond which the impulsive friction and noise is not applied ($f = 0$). In practice, one uses the short-range pair list that is constructed already for the determination of forces. The distance dependence can be chosen arbitrarily; the original DPD[12,13] chooses a linear dependence between 1 ($r = 0$) and 0 ($r = r_c$). By combining the various methods and adjusting their damping and distance dependencies, the viscosity, diffusion, and thermostat behavior can be separately influenced.[25]

After determining the *change* in the relative velocity due to the impulsive friction and noise, this change is distributed over the two particles such that the c.o.m. is conserved.

The algorithm is equal to the constrained Langevin algorithm of section 3.3, except that step 6 is replaced by the sequential application of all pairwise impulsive events. The resulting velocities are v_i', which enter step 7 of the algorithm. Step 6 now reads as follows.

Select pairs i,j that will be subjected to impulsive friction and noise. This pair selection can be done in several ways. In principle, all neighbors from the list can be selected (this would correspond to the original DPD procedure), but it is sufficient and much more efficient to select only one (or a few) neighbor(s) per particle. The selection can be made at random, but it can also be based on a distance-weighted probability, e.g., proportional to $1 - r_{ij}/r_c$. A selected pair can be subjected to friction and corresponding noise, with the friction either isotropically in the direction of the velocity itself (iso), parallel to $\mathbf{r}_{ij}$ (par), or in a direction perpendicular to $\mathbf{r}_{ij}$ (perp). In the following, it is assumed that a particular choice has been made, but it is also possible to combine more than one choice. Different choices can be applied to the same particle pair, but each choice can also be applied to a different pair.

For each selected pair i,j with velocities $\mathbf{v}_i$ and $\mathbf{v}_j$, do the following:

1. Choose the *velocity reduction factor* f (either f_{iso} or f_{par} or f_{perp}) based on the interparticle distance r_{ij}. Note that distance dependence can be achieved in two ways: either by making f distance dependent or by using a distance-dependent weight in the pair selection procedure. Do not use both at the same time! If the pair selection has been based on a distance-dependent probability, the factors f can be taken as equal for all pairs. Note that the coordinates to be used for the determination of f should—strictly speaking—be taken at the half-step $t + (1/2)h$, i.e., after step 3a in Figure 1. Using $r(t)$ instead will have a negligible effect.
2. Determine the *velocity noise factor* g, defined as

$$g = \sqrt{f(2 - f)k_B T_{ref}/\mu} \tag{23}$$

where

$$\mu = \frac{m_i m_j}{m_i + m_j} \tag{24}$$

dx.doi.org/10.1021/ct3000876 | J. Chem. Theory Comput. 2012, 8, 3637−3649

is the reduced mass of the two particles. If f has been made distance dependent, this distance dependency should be contained in f in eq 23. If the pair selection has been based on a distance-dependent probability, eq 23 can be used *as is*.

3. Construct the relative velocity vector $\mathbf{v}$ of the selected pair:

$$\mathbf{v} = \mathbf{v}_i - \mathbf{v}_j \tag{25}$$

4. If iso:
   a. Choose three random numbers $\xi = (\xi_1,\xi_2,\xi_3)$ from a standard normal distribution (mean = 1, sd = 1).
   b. Construct the vector:

$$\Delta\mathbf{v} = -f\mathbf{v} + g\xi \tag{26}$$

Proceed to step 5.

If par:

   a. Construct a unit vector $\mathbf{e}_1$ in the interparticle direction:

$$\mathbf{e}_1 = \frac{\mathbf{r}_{ij}}{|r_{ij}|} \tag{27}$$

where $\mathbf{r}_{ij} = \mathbf{r}_i - \mathbf{r}_j$.

   b. Determine the component of $\mathbf{v}$ in the interparticle direction:

$$v_{\text{par}} = \mathbf{v}\cdot\mathbf{e}_1 \tag{28}$$

   c. Choose one random number ξ from a standard normal distribution (mean = 1, sd = 1).
   (d) Construct the vector

$$\Delta\mathbf{v} = (-fv_{\text{par}} + g\xi)\mathbf{e}_1 \tag{29}$$

Proceed to step 5.

If perp:

   a. Construct a unit vector $\mathbf{e}_1$ in the interparticle direction:

$$\mathbf{e}_1 = \frac{\mathbf{r}_{ij}}{|r_{ij}|} \tag{30}$$

where $\mathbf{r}_{ij} = \mathbf{r}_i - \mathbf{r}_j$.

   b. Construct the velocity component perpendicular to $\mathbf{e}_1$:

$$\mathbf{v}_{\text{perp}} = \mathbf{v} - (\mathbf{v}\cdot\mathbf{e}_1)\mathbf{e}_1 \tag{31}$$

   c. Construct a unit vector in the direction of $\mathbf{v}_{\text{perp}}$:

$$\mathbf{e}_2 = \frac{\mathbf{v}_{\text{perp}}}{|v_{\text{perp}}|} \tag{32}$$

   d. Construct a unit vector $\mathbf{e}_3$ perpendicular to $\mathbf{e}_1$ and $\mathbf{e}_2$:

$$\mathbf{e}_3 = \mathbf{e}_1 \times \mathbf{e}_2 \tag{33}$$

   e. Choose two random numbers ξ_2 and ξ_3 from a standard normal distribution (mean = 1, sd = 1).
   f. Construct the vector

$$\Delta\mathbf{v} = -f\mathbf{v}_{\text{perp}} + g(\xi_2\mathbf{e}_2 + \xi_3\mathbf{e}_3) \tag{34}$$

Proceed to step 5.

5. Distribute the relative velocity change over the two particles:

$$\mathbf{v}_i \leftarrow \mathbf{v}_i + \frac{\mu}{m_i}\Delta\mathbf{v} \tag{35}$$

$$\mathbf{v}_j \leftarrow \mathbf{v}_j - \frac{\mu}{m_j}\Delta\mathbf{v} \tag{36}$$

In this way, the velocities of the particles are updated while the total momentum $m_i\mathbf{v}_i + m_j\mathbf{v}_j$ is conserved.

Note that the particle velocities are updated after each impulsive event, not at the end of each step. This is necessary, as a single particle may be involved in more than one pair event; first adding the velocity changes and updating the velocities with the sum of the velocity changes gives erroneous results.

The equations for pairwise friction and noise are the same as for a system without constraints, despite the fact that $\langle v^2\rangle \neq k_BT/\mu$ per degree of freedom, when one or both of the particles in a pair is involved in constraints. Similar to the simple Langevin thermostat applied to systems with constraints, for small frictions the excess velocities in the constraint directions are removed by the application of constraints after the impulsive step; this also removes the excess kinetic energy.

4.1. Thermostat Behavior. We ask how the total energy changes by the application of friction and noise as described above. The total energy change distributes itself over kinetic and potential energy and leads to a temperature change determined by the specific heat of the system. Thus, we obtain a differential equation for the time-dependent behavior of the temperature, similar to the case of Langevin dynamics treated in section 2.2. As we shall see below, also in the case of pairwise friction and noise, the temperature appears to relax with a first-order process toward the reference temperature. The derivation that follows is valid for the nonconstraint case.

The energy change concerns one, two, or three degrees of freedom, related to the relative velocity of two particles, with reduced mass $\mu = m_im_j/(m_i + m_j)$. The dimensionality $d = 1$ when a component in one direction is considered as in the par case; $d = 2$ when a component in a plane is considered as in the perp case, while $d = 3$ in the iso case.

The derivation follows exactly the Langevin case (section 2.2). The energy change due to the application of one impulsive friction and noise event in d dimensions of the relative velocity vector of a selected pair is given by

$$\Delta E = \frac{1}{2}\mu(v + \Delta v)^2 - \frac{1}{2}\mu v^2 \tag{37}$$

$$= \frac{1}{2}df(2 - f)k_B(T_{\text{ref}} - T) \tag{38}$$

where T is given by

$$T = \frac{\mu}{k_B}\langle v^2\rangle \tag{39}$$

Using

$$\Delta T = \frac{\Delta E}{C_V} \tag{40}$$

valid for the usual case where the rate constant of the thermostat is smaller than the intrinsic exchange rate between

kinetic and potential energy, we arrive at the rate equation for the temperature:

$$\frac{dT}{dt} = \frac{k_B d}{2C_V} \frac{\sum f(2-f)}{h} (T_{ref} - T) \tag{41}$$

where the sum is to be taken over all d-dimensional events per time step. This is a first-order decay toward the reference temperature with the rate constant

$$k_{th} = \frac{dk_B}{2C_V} \frac{\sum f(2-f)}{h} \tag{42}$$

We note that in the case of very strong thermostats, $2C_V/k_B$ should be replaced by the total number of degrees of freedom (see remark at the end of section 2.2).

In the particular case that for all particles in the system one pair is selected in every time step and the velocity reduction factor f is weighted by a distance-dependent factor, i.e. $1 - r/r_c$, where r_c is a cutoff range used in the neighbor selection, the resulting equation for the time constant of the thermostat is

$$k_{th} = \frac{k_B d}{2c_V} \left(\frac{2f\langle (1 - r/r_c)\rangle - f^2 \langle (1 - r/r_c)^2 \rangle}{h} \right) \tag{43}$$

where c_V is the specific heat per particle and d is the dimensionality of the applied friction and noise:

for iso $d = 3$
for par $d = 1$
for perp $d = 2$

The averages are to be taken over the randomly selected pairs. Given a radial distribution function $g(r)$ and a cutoff radius r_c, such averages are determined from

$$\langle h(r)\rangle = \frac{\int_0^{r_c} h(r)\, g(r) r^2 \, dr}{\int_0^{r_c} g(r) r^2 \, dr} \tag{44}$$

5. EFFECTIVE FRICTION RATE AND DIFFUSION

The effective friction rate imposed by impulsive velocity reductions is not only a function of the velocity reduction factor f but also of the time step, the dimensionality of the event, the number of events per time step, and the distance-dependent weight factor. In order to compare different applications, we define for each case an *effective friction rate* γ_{eff}.

For the Langevin application, where a velocity reduction to $(1 - f)v$ is applied to every degree of freedom at every time step, we defined an effective friction rate in eq 19:

$$\gamma_{eff} = -\frac{\ln(1-f)}{h} \tag{45}$$

The effective gamma is related to the diffusion coefficient D_0 in the absence of systematic forces. The diffusion coefficient of particles in a fluid is given by[11]

$$D = \int_0^\infty \langle v(0)\, v(t)\rangle \, dt = \frac{k_B T}{m} \int_0^\infty \overline{C_{vv}(t)} \, dt \tag{46}$$

where $\overline{C_{vv}(t)}$ is the normalized velocity autocorrelation function

$$\overline{C_{vv}(t)} = \frac{1}{\langle v^2 \rangle} \langle v(0) v(t)\rangle \tag{47}$$

Here, averaging is both over the ensemble and over the time origin. In the case of continuous friction with rate γ and in the absence of systematic forces (ideal gas), the normalized velocity correlation function equals $\exp(-\gamma t)$, with integral $1/\gamma$. The inverse diffusion coefficient is proportional to γ and given by

$$D_0^{-1} = \frac{m}{k_B T} \gamma \tag{48}$$

In the case of impulsive damping, the normalized velocity correlation function equals the dotted line in Figure 2 rather

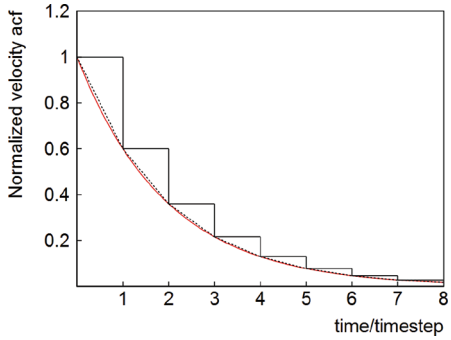

Figure 2. Normalized velocity autocorrelation functions for continuous friction (red line: exponential decay) and for impulsive friction (dotted line: polylinear decay), in the absence of systematic forces. The drawn step function indicates the velocity reduction at the end of each time step. For this example, $f = 0.4$.

than the drawn exponential function valid for continuous damping. Its integral equals $(1 - (1/2)f)h/f$, rather than $1/\gamma$. The deviation is of second order and very small, which means that eq 45 can be used to predict diffusion coefficients in the ideal gas case. Note that the factor $(1 - (1/2)f)$ arises from averaging over time origins within a time step.

For the pairwise application to unconstrained systems, we expect the same equation to be valid when the total number of degrees of freedom affected per time step equals the total number of degrees of freedom in the system, i.e., equal to three times the number of particles. When friction and noise are applied to one pair per particle, this implies for DPD thermostats that the effective friction rate γ_{eff} is given by

$$\gamma_{eff} = -\frac{\ln\left(1 - \frac{1}{3}\langle 1 - r/r_c\rangle f d\right)}{h} \tag{49}$$

where d is the dimensionality of the DPD friction, and the distance-dependent factor by which f has been multiplied has been taken into account. We note that for homogeneous distributions $\langle 1 - r/r_c\rangle = 1/4$, irrespective of the value of r_c.

For the application of impulsive friction and noise to systems with constraints, the situation is more complex, but the same eqs 45 and 49 for the effective gamma apply. Suppose there are n particles with n_c holonomic constraints, so there are $3n - n_c$ degrees of freedom. If impulsive friction and noise are applied to a particle or to a pair that is involved in constraints, part of the velocity change (and hence energy change) is removed by the constraints. On average, the remaining fraction of the energy change equals $(3n - n_c)/(3n)$. If applied (per time step) to three dimensions of n pairs, effectively only $3n - n_c$ degrees of freedom are modified. Thus, the damping is as effective as in the unconstrained case. In summary, eqs 45 and 49 describe the effective friction rate for Langevin and DPD dynamics, respectively, both for unconstrained and constrained systems.

6. COMPUTATIONAL DETAILS

6.1. Simulation Details. The algorithms presented in the previous sections were implemented in the GROMACS program package,[26] version 4.0.7, using parallelization based on domain decomposition.

Three types of systems were used to test performance of the investigated coupling schemes: ideal gas, MARTINI[27] water, and SPC/E[28] water. All simulations were performed in a periodic cubic box with dimensions longer than twice the cutoff distance. A cutoff distance for both nonbonded interactions and DPD thermostat was set at 1.2 nm for ideal gas and MARTINI water systems and 0.9 nm for the SPC/E water system. For MARTINI, a potential shift function was applied,[29] with a switch value of 0.9 to remove cutoff effects. In SPC/E water simulations, we used the particle-mesh-Ewald (PME) method to calculate long-range coulomb interactions above 0.9 nm. The neighbor list was updated every step in order to remove any deviations due to computational errors. In all simulations, a time step of 2 fs was used. Bond distances in the SPC/E water model were constrained using the SETTLE algorithm.[22] For equilibration, weak pressure coupling[5] was applied with a time constant of 2.0 ps and a reference pressure of 1 bar; production runs were performed under constant volume conditions. The reference temperature was set to 320 K for ideal gas and MARTINI water systems and to 300 K for the SPC/E water system.

The ideal gas and MARTINI water systems consisted of 3200 particles with a mass of 72 u in a cubic box of $(7.28856\ \mathrm{nm})^3$; the SPC/E system consisted of 1728 molecules in a cubic box of $(3.7252\ \mathrm{nm})^3$. The initial velocities of the particles were obtained from a Maxwell−Boltzmann distribution corresponding to the chosen initial reference temperature. Simulations were either 10 ns or 50 ps long, for diffusion and thermal rate calculations, respectively.

For the computation of the diffusion coefficient, we used the mean square displacement (MSD) and applied the Einstein relation $D = \langle r^2(t)\rangle/(6t)$. The diffusion coefficient was calculated by least-squares fitting a straight line through the MSD from 500 ps to 2 ns. Thermal rate constants were determined from least-squares fits to a single exponential of the temperature after switching the reference temperature at time $t = 0$ from 350 to 320 K (ideal gas and MARTINI water) or from 330 to 300 K (SPC/E water). Each case was repeated eight times, yielding eight independent determinations k_i of the rate constant; we report the averages $\bar{k}$ with standard uncertainty σ computed from $\sigma^2 = \sum_{i=1}^{8}(k_i - \bar{k})^2/56$.

6.2. Performance. We ran efficiency measurements on a workstation with a Dual Core AMD Opteron 865 (1800 MHz) processor. The comparison was done on a Martini water system with 3200 CG particles and with a time step of 10 fs, using Gromacs version 4.0.7. For the DPD case, we choose iso—the other DPD algorithms have the same order of computational complexity. For Langevin dynamics, we compared the "new" impulsive algorithm with the "old" algorithm available in Gromacs, which is based on the integration of continuous friction,[4] and with pure MD without and with a global thermostat. For iso, we compared the random selection of one pair per particle with the selection of all pairs from the whole neighbor list of each particle. In Table 1, the "speed" is reported as the number of nanoseconds simulated per day (24 h).

From these efficiency experiments, we can conclude that all our new algorithms perform better than the existing algorithms from the literature or those implemented in Gromacs. For pairwise applications, it is especially rewarding, with a 7-fold efficiency gain, to apply friction and noise to only one random pair per particle.

Table 1

method	ns/day
MD, no thermostat	69.90
MD, Berendsen thermostat	69.81
SD, Langevin, "old"	59.79
SD, Langevin, "new"	67.44
SD pairwise iso, one pair per particle	55.21
SD pairwise iso, n^a pairs per particle	7.47

[a] n is length of neighbor list; complexity comparable to traditional DPD.

7. RESULTS

7.1. Ideal Gas. First, we checked the influence of the Langevin and the different DPD thermostats on the radial distribution function and the temperature for the chosen ideal gas system. By applying Langevin dynamics and all three variants of DPD in a scheme in which the friction coefficient f/h was kept constant to 1 ps^{-1} and the time step was varied between 2 and 100 fs, we found the temperature and the radial distribution functions to be independent of the time step used. This is similar to that observed by Peters.[17] In Figure 3a, equivalent results, where the time step is kept constant at 2 fs and the friction rate is varied, are shown for the "iso" case of a DPD coupling. The radial distribution remained homogeneous within statistical accuracy for various values of the friction rate γ. The temperature was monitored not only for the ideal gas but also for MARTINI water and SPC/E water for a gamma ranging up to 60 ps^{-1}. The temperature did not deviate from the reference temperature within statistical error (results not shown), except for SPC/E water (which involves constraints) for DPD friction rates above 10 ps^{-1}. The latter could be due to the constraint correction to the velocity change. Further investigation of this effect showed that the deviation was reduced by using a smaller time step and also by applying friction and noise to more than one pair per step. Figure 3b shows the temperature deviation for the "iso" DPD case for SPC/E water, using up to 12 pairs per step and plotted against γ_{eff} using eq 49. For $\gamma_{\mathrm{eff}} < 10\ \mathrm{ps}^{-1}$ (a practical upper limit), the effect is small in all cases, but it is very much smaller if several pairs are used.

For the ideal gas, we studied the influence of friction strength on diffusion. For the ideal gas, the only damping of the velocity is due to the imposed friction, implying that the diffusion coefficient should follow from the effective damping according to eq 48 when the appropriate γ_{eff} from either eq 45 or 49 is used. The inverse of the diffusion coefficient should be proportional to the (effective) friction rate γ_{eff}:

$$D^{-1} = C\gamma_{\mathrm{eff}};\ C = \frac{m}{k_{\mathrm{B}}T} = 27.1\ \mathrm{ps}^2\ \mathrm{nm}^{-2} \tag{50}$$

In Figure 4a, D^{-1} is plotted versus the friction rate, eq 45, for the Langevin case; the agreement with theoretical predictions is perfect. For the DPD case shown in Figure 4b, eq 49 is used for the friction rate; the theoretical prediction corresponds fairly closely to the measured values with slight deviations at higher friction rates, notably for the "par" case.

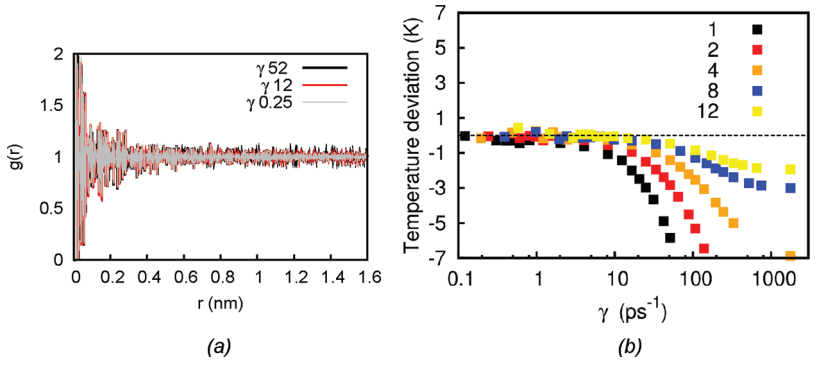

Figure 3. Overall behavior of algorithms. (a) Radial distribution functions for ideal gas simulated with the "iso" coupling scheme with three friction rates (black line γ = 52 ps^{-1}, red line γ = 12 ps^{-1}, and gray line γ = 0.25 ps^{-1}; time step 2 fs.). (b) Deviation from the reference temperature for equilibrium DPD simulations with the "iso" coupling scheme on SPC/E water, as a function of γ_{eff} (see text) for 1, 2, 4, 8, and 12 pairs per step.

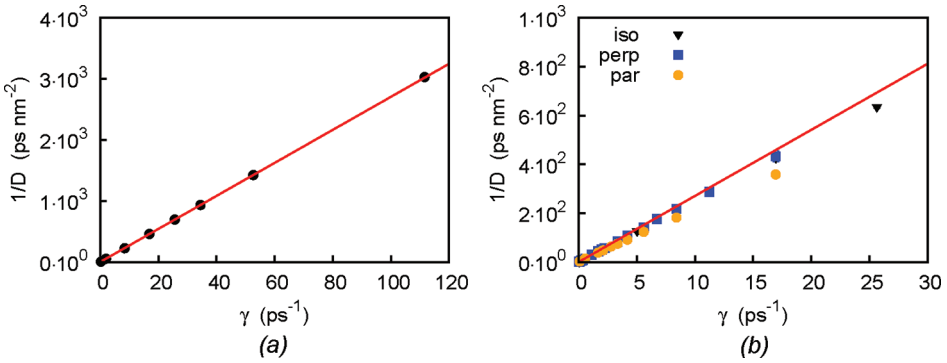

Figure 4. (a) Inverse diffusion coefficient versus friction rate for ideal gas simulated with impulsive Langevin algorithm. Black dots, simulations; red line, theory. Errors are smaller than the line width of the graph. (b) Inverse diffusion coefficient versus effective friction rate for "iso", "perp", and "par" DPD coupling schemes utilized in an ideal gas system. Red line, theory; black inverted triangles, "iso"; blue squares, "perp"; and yellow dots, "par".

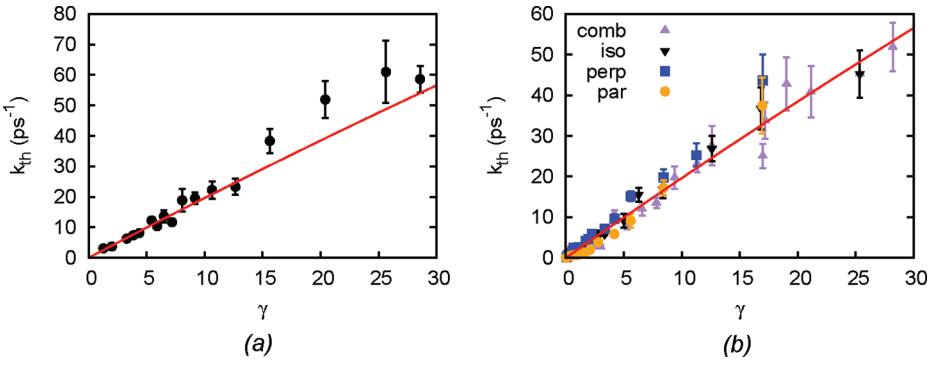

Figure 5. (a) Thermal relaxation rate versus friction rate for ideal gas simulated with impulsive Langevin algorithm. Black dots simulations, red line theory. (b) The same for "iso", "par", and "perp" DPD coupling schemes used with the ideal gas system. Red line, theory; black inverted triangles, "iso"; blue squares, "perp"; yellow dots, "par"; and purple triangles, combinations of the last two couplings.

Finally, we determined the thermal relaxation rate constant for all variants of the impulsive friction. The equation for the thermal rate constant k_{th} (see section 2.2) is for an ideal gas with Langevin friction:

$$k_{th} = \frac{f(2-f)}{h} = \frac{1-\exp(-2\gamma_{eff}h)}{h} \tag{51}$$

where $\gamma_{eff} = -[\ln(1-f)]/h$ as in eq 45. Figure 5a compares the theoretical prediction with the simulated thermal rate constants. The agreement is reasonable, with slight deviations at high friction rates.

For the pairwise DPD-type application, using one pair interaction of dimensionality d (par: d = 1; perp: d = 2; iso: d = 3) per particle per step, the equation for the thermal rate constant is (see section 4.1):

$$k_{th} = \frac{d}{3}\left(\frac{2f\langle 1 - r/r_c\rangle - f^2\langle (1-r/r_c)^2\rangle}{h}\right) \tag{52}$$

This equation can be simplified by expressing the friction again as an effective friction rate, eq 49, yielding the same relation as in the Langevin case:

$$k_{th} \approx \frac{1-\exp(-2\gamma_{eff}h)}{h} \tag{53}$$

dx.doi.org/10.1021/ct3000876 | J. Chem. Theory Comput. 2012, 8, 3637−3649

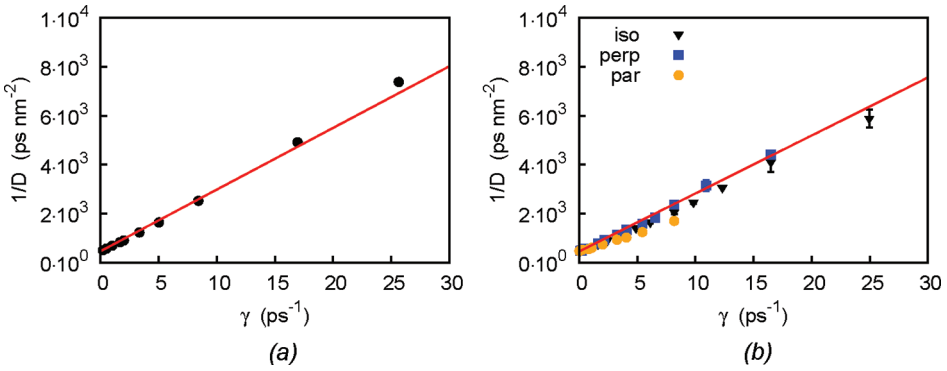

Figure 6. (a) Inverse diffusion coefficient versus friction rate for MARTINI coarse grained water, simulated with impulsive Langevin algorithm. Black dots, simulations; red line, fit to ($D_{\text{intr}}^{-1} + C\gamma$; C = 250 ps^2 nm^{-2}). (b) Same for "iso", "par", and "perp" DPD coupling schemes used with the MARTINI coarse grained water system. Black inverted triangles, "iso"; blue squares, "perp"; yellow dots, "par"; red line, fit to ($D_{\text{intr}}^{-1} + C\gamma$; C = 250 ps^2 nm^{-2}).

Equation 53 is accurate for small γ, or for any γ if the difference between $\langle(1 - r/r_c)^2\rangle$ and $\langle(1 - r/r_c)\rangle^2$ can be neglected.

Figure 5b shows the results. For all cases, the results agree within experimental error with the theory.

7.2. MARTINI Coarse-Grained Water. In the presence of an intrinsic diffusion coefficient, there is no reliable theory for the behavior of the diffusion coefficient as a function of applied friction. One might naively suppose that internal and external friction would be additive, i.e., that the inverse diffusion coefficient would be the sum of the inverse intrinsic diffusion coefficient and the inverse diffusion coefficient of the ideal gas. However, this assumption leads to a much higher diffusion coefficient than is actually observed. It turns out that the observed inverse diffusion coefficient obeys the following empirical linear relation to γ:

$$\frac{1}{D} = \frac{1}{D_{\text{intr}}} + C\gamma_{\text{eff}} \tag{54}$$

where C is a proportionality constant with dimension ps^2 nm^{-2}, which depends on the nature of the intrinsic interaction between the particles. The inverse diffusion coefficients are given in Figure 6a for the Langevin case and in Figure 6b for the DPD case. In both cases, the proportionality constant C = 250 ps^2 nm^{-2}. We also computed the diffusion coefficients when the potential energy function was decreased by a constant factor between 0 and 1; the factor C appeared to be proportional to the strength of the interparticle forces.

For prediction of the thermal rate, the following properties of MARTINI water at 320 K are needed: c_V = 0.0234(3) kJ mol^{-1} K^{-1}, $\langle 1 - r/r_c\rangle$ = 0.24336, and $\langle(1 - r/r_c)^2\rangle$ = 0.089437. For the Langevin case, the equation for the thermal rate constant k_{th} (see section 2.2) is for a fluid:

$$k_{\text{th}} = \frac{3k_B}{2c_V}\frac{f(2-f)}{h} = \frac{3k_B}{2c_V}\frac{[1 - \exp(-2\gamma h)]}{h} \tag{55}$$

where $\gamma = -[\ln(1 - f)]/h$. As MARTINI water is governed by an intrinsic potential, c_V is larger than its ideal-gas value of $3k_B/2$; in fact, $3k_B/(2c_V)$ = 0.533. Thus, we expect a "slow" thermostat at low friction rates and an almost twice as large "fast" thermostat at high friction rates (see section 2.2). The crossover point is expected near the time when the autocorrelation function of the kinetic energy (or the temperature) has decayed, i.e., roughly between 0.1 and 0.2 ps, as shown in Figure 7.

Figure 8a compares the theoretical prediction with the simulated thermal rate constants. The agreement with theory is very good. The full-drawn line gives the "slow" behavior, and the broken red line indicates the "fast" behavior. The crossover time between the two regimes occurs around γ = 10, or 0.1 ps, which is in the expected range.

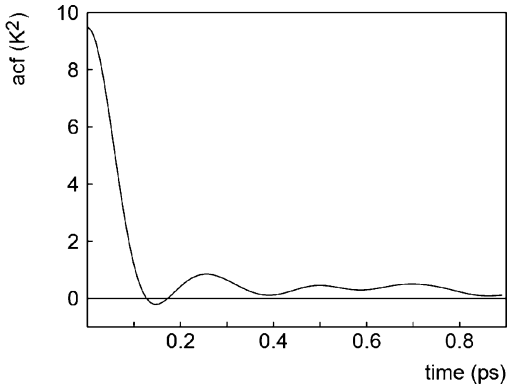

Figure 7. Autocorrelation function of the temperature for MARTINI coarse-grained water at 320 K, showing the time course of the exchange between kinetic and potential energy.

For DPD, with one pair selected per particle per time step, the thermal rate is similarly modified; eq 53 now becomes

$$k_{\text{th}} = \frac{3k_B}{2c_V}\frac{[1 - \exp(-2\gamma_{\text{eff}}h)]}{h} \tag{56}$$

Figure 8b shows that also in the DPD cases the experimental values agree with eq 56 for "slow" friction rates (γ < 10 ps^{-1}) and with eq 53 for "fast" friction rates.

7.3. SPC/E Water. This test case differs from MARTINI water in that we now consider a system with constraints. The impulsive friction and noise is applied once per time step to every *atom* in the Langevin case, or to one pair involving every atom in the DPD cases. The individual velocity changes are much larger in the DPD cases than in the Langevin case for the same effective friction rate.

Figure 9 plots the inverse diffusion coefficients versus γ. Also here, the inverse D is proportional to the effective friction rate γ. The intrinsic inverse diffusion coefficient equals 420 ps nm^{-2}, and the proportionality constant C equals 46 ps^2 nm^{-2} for the Langevin case and 24 ps^2 nm^{-2} for the DPD cases, much larger than the ideal gas value of 7.2 ps^2 nm^{-2} (m = 18 u, T = 300 K). Contrary to the MARTINI system, here the influence of the friction rate on the diffusion coefficient is less for the DPD case than for the Langevin case.

dx.doi.org/10.1021/ct3000876 | J. Chem. Theory Comput. 2012, 8, 3637−3649

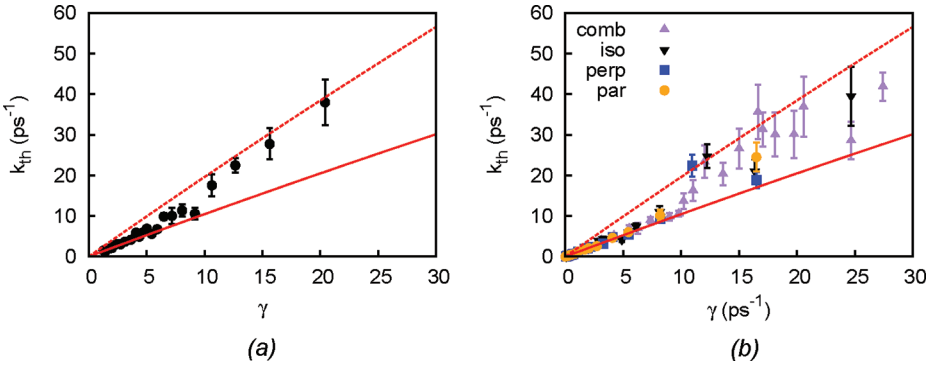

Figure 8. (a) Thermal relaxation rate versus friction rate for MARTINI coarse grained water, simulated with impulsive Langevin algorithm. Black dots simulations; red lines theory, full-drawn for "slow" and dotted for "fast" thermostats. (b) The same for "iso", "par", and "perp" DPD coupling schemes. Black inverted triangles, "iso"; blue squares, "perp"; yellow dots, "par"; and purple triangles, combinations of the last two couplings. Red lines, theory, full-drawn for "slow" and dotted for "fast" thermostats.

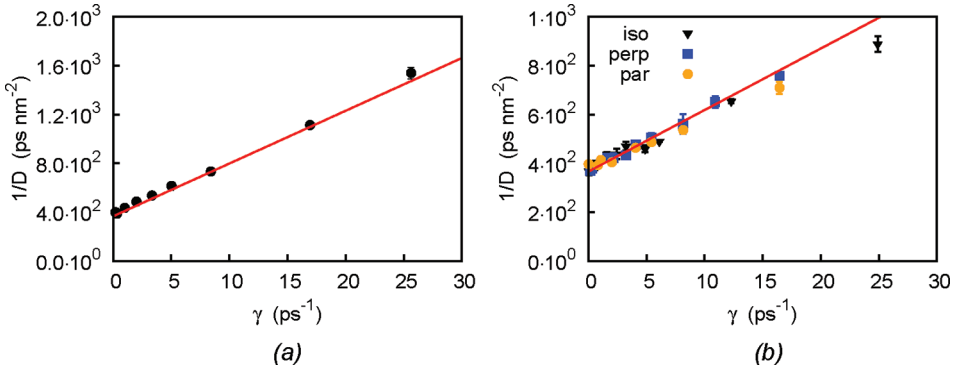

Figure 9. (a) Inverse diffusion coefficients versus the friction rate for the atomistic SPC/E water system, simulated with impulsive Langevin algorithm. Black dots, simulation results; red line, fit to ($D_{\mathrm{intr}}^{-1} + C\gamma$; C = 46 ps^2 nm^{-2}). (b) Same for "iso", "par", and "perp" DPD coupling schemes. Inverted triangles, "iso"; blue squares, "perp"; and yellow dots, "par". Red line fit to ($D_{\mathrm{intr}}^{-1} + C\gamma$; C = 24 ps^2 nm^{-2}).

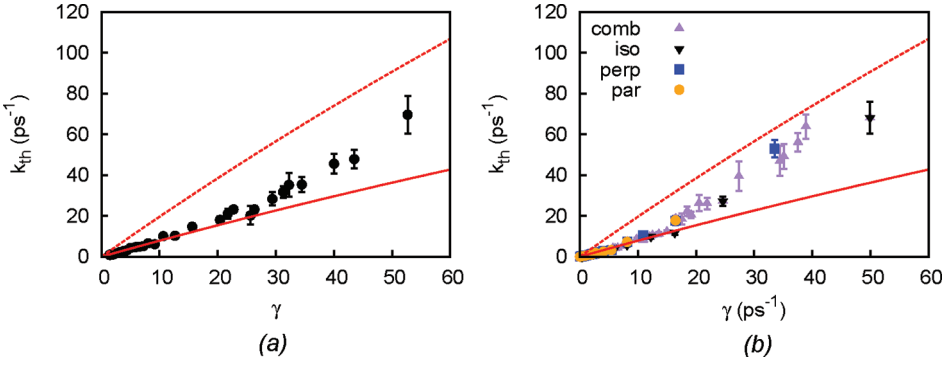

Figure 10. (a) Thermal relaxation rate versus friction rate for the atomistic SPC/E water system, simulated with impulsive Langevin algorithm. Black dots, simulations; red lines, theory, full-drawn for "slow" and dotted for "fast" thermostats. (b) Same for "iso", "par", and "perp" DPD coupling schemes. Black inverted triangles, "iso"; blue squares, "perp"; yellow dots, "par"; and purple triangles, combinations of last two couplings. Red lines, theory, full-drawn for "slow" and dotted for "fast" thermostats.

For prediction of the thermal rate, the following properties of SPC/E water at 300 K are needed: c_V = 0.0623 kJ mol^{-1} K^{-1}, $\langle 1 - r/r_c \rangle$ = 0.2429, $\langle (1 - r/r_c)^2 \rangle$ = 0.094038. The thermal relaxation rates (Figure 10) closely follow the theory. The transition to the "fast" rate sets in above 20 ps^{-1} (below 50 fs) and reaches its full rate (three times the "slow" rate) beyond the scale of the graph.

8. DISCUSSION AND CONCLUSIONS

In this article, we have shown that the application of impulsive friction and noise, as introduced by Peters,[17] provides a valid implementation for Markovian stochastic dynamics with predictable thermostat behavior. This is true both for the traditional particle-based simple Langevin dynamics and for the Galilean-invariant pairwise application of friction and noise as are typical for Dissipative Particle Dynamics (DPD). We presented the leap-frog algorithm and allowed the pairwise friction and noise to be chosen either in the direction of the interpair vector ("par"), perpendicular to it ("perp"), or independent of it ("iso"). The algorithms apply both to unconstrained systems and to systems with holonomic constraints. In the latter case, friction and noise are applied

dx.doi.org/10.1021/ct3000876 | J. Chem. Theory Comput. 2012, 8, 3637−3649

as if the constraints did not exist; the constraint algorithm automatically corrects for velocity changes along the constraints. We have indicated how pressure evaluations can be implemented.

In the pairwise application, there is a wide choice of particle pairs to which friction and noise may be applied. Using a single pair per particle per time step is computationally very efficient, but could—for very high friction rates—introduce errors in the presence of constraints. These errors are substantially reduced by allowing more than one pair per particle, be it at the expense of computational efficiency.

In eqs 45 and 49, we have defined an effective friction rate γ_{eff} for all cases, which provides a comparable measure for the strength of the friction. The "thermal rate" k_{th}, which is a measure for the strength of the thermostat, as it equals the rate constant for the first-order decay of the difference between system temperature and reference temperature, is directly related to γ_{eff}. The relation is given in eq 53 or 56:

$$k_{\text{th}} = A\frac{[1 - \exp(-2\gamma_{\text{eff}}h)]}{h} \tag{57}$$

where $A = 1$ for "fast" thermostats and $A = 3k_B/(2c_V)$ for "slow" thermostats. Here, "fast" means that the rate of exchange between kinetic energy and the thermal bath is faster than the intrinsic exchange between kinetic and potential energy in the system, so that the system has no time to redistribute kinetic energy changes over kinetic and potential energy pools. "Slow" means that the system does have the time to equilibrate between the two pools. For an ideal gas, there is no potential energy, and hence $A = 1$. In practice, a thermostat will be employed to correct for long-term drift due to algorithmic errors, and its strength will be chosen in the "slow" regime (as $\gamma_{\text{eff}} < 5$ ps^{-1} in our examples). Note that in this limit, $\gamma_{\text{eff}}h \ll 1$, and eq 57 reduces to $k_{\text{th}} = 2A\gamma_{\text{eff}}$.

What are the advantages and disadvantages of the application of impulsive friction and noise? First, the phase space distribution remains canonical, which cannot be guaranteed for weak-coupling global thermostats.[5] Second, the temperature response is a smooth first-order decay, which avoids many problems of extended-system global thermostats.[9,11] Third, as in DPD, pairwise application assures the conservation of linear momentum on a fairly local scale, allowing application in cases where adherence to the Navier–Stokes relations in the macroscopic limit is essential. Fourth, the local character of the pairwise application allows one to impose and maintain spatial temperature gradients, or different temperatures for different subsystems. Fifth, the choice in parameters allows a kind of "fine-tuning" of dynamic properties.

Knowledge of the behavior as a thermostat is but the first step in a full control of the dynamic effects of applied friction and noise. Ideally, if the influence on transport properties as shear viscosity, diffusion, and thermal conductivity were predictable, the user could fine-tune the system to achieve desired properties. For example, one can choose the pairwise application in three flavors (iso, perp, par); with equal thermostat strength, the "perp" form increases shear viscosity the most and the "par" form increases it the least. In a preliminary evaluation, we found the viscosity increase for equal γ_{eff} to be in the ratio iso/perp/par = 5:6:3. If a viscosity increase is desired without any thermostatting action, a pairwise form of Stochastic Rotational Dynamics (SRD)[30,31] could be implemented.

Unfortunately, the prediction of the influence of friction and noise on dynamic properties of systems with internal interactions is not straightforward at all. As we saw, the diffusion coefficient could be predicted precisely for the ideal gas, but for both coarse-grained and atomic water theoretical predictions are not (yet) possible. Even the linear relation between the inverse diffusion coefficient and the additional friction rate is a purely empirical observation. These issues are the subject of further study.

AUTHOR INFORMATION

Corresponding Author

*E-mail: H.J.C.Berendsen@rug.nl.

Notes

The authors declare no competing financial interest.

ACKNOWLEDGMENTS

We are grateful to one of the reviewers, Dr. E. A. F. J. Peters of the Technical University, Eindhoven, for his comments, pointing out the inadequacy of the Andersen thermostat if applied to selected particles in systems with constraints. These comments have led to substantial improvements in the manuscript.

DEDICATION

We are proud to dedicate the present article—which describes and evaluates a modern version of stochastic algorithms—to Wilfred van Gunsteren on the occasion of his 65th birthday. As mentioned in the Introduction, Wilfred was deeply involved in the design and application of stochastic algorithms of the Langevin type in the 1980s. His sophisticated algorithm, based on integration of the equations of motions with noise over a time step, was incorporated into GROMOS at the time and has served the community well for decades. We wish Wilfred many happy years to come, within or beyond science!

REFERENCES

(1) van Gunsteren, W. F.; Berendsen, H. J. C.; Rullmann, J. A. C. *Mol. Phys.* **1981**, *44*, 69–95.
(2) van Gunsteren, W. F.; Berendsen, H. J. C. *Mol. Phys.* **1982**, *45*, 637–647.
(3) van Gunsteren, W. F.; Berendsen, H. J. C. In *The Physics of Superionic Conductors and Electrode Materials*; Perram, J. W., Ed.; Plenum: New York, 1983; NATO ASI Series, *B 92*, pp 241–256.
(4) van Gunsteren, W. F.; Berendsen, H. J. C. *Mol. Simul.* **1988**, *1*, 173–185.
(5) Berendsen, H. J. C.; Postma, J. P. M.; van Gunsteren, W. F.; DiNola, A.; Haak, J. R. *J. Chem. Phys.* **1984**, *81*, 3684–3690.
(6) Morishita, T. *J. Chem. Phys.* **2000**, *113*, 2976–2982.
(7) Harvey, S. C.; Tan, R. K. Z.; Cheatham, T. E. *J. Comput. Chem.* **1998**, *19*, 726–740.
(8) Bussi, G.; Donadio, D.; Parrinello, M. *J. Chem. Phys.* **2007**, *126*, 04101.
(9) Hoover, W. G. *Phys. Rev.* **1985**, *A31*, 1696–1697.
(10) Martyna, G. J.; Tuckerman, M. E.; Klein, M. L. *J. Chem. Phys.* **1992**, *97*, 2635–2643.
(11) Berendsen, H. J. C. *Simulating the Physical World, A Hierarchy of Models for Simulation*; Cambridge University Press: Cambridge, U. K., 2007.
(12) Hoogerbrugge, P. J.; Koelman, J. M. V. A. *Europhys. Lett.* **1992**, *19*, 155–160.
(13) Koelman, J. M. V. A.; Hoogerbrugge, P. J. *Europhys. Lett.* **1993**, *21*, 363–368.
(14) Español, P.; Warren, P. *Europhys. Lett.* **1995**, *30*, 191–196.
(15) Allen, M. P. *Mol. Phys.* **1980**, *40*, 1073–1087.

(16) Nikunen, P.; Karttunen, M.; Vattulainen, I. *Comput. Phys. Commun.* **2003**, *153*, 407−423.
(17) Peters, E. A. F. J. *Europhys. Lett.* **2004**, *66*, 311−317.
(18) Andersen, H. C. *J. Chem. Phys.* **1980**, *72*, 2384−2393.
(19) Lowe, C. P. *Europhys. Lett.* **1999**, *47*, 145−151.
(20) Ryckaert, J. P.; Ciccotti, G.; Berendsen, H. J. C. *J. Comput. Phys.* **1977**, *23*, 327−341.
(21) Hess, B.; Bekker, H.; Berendsen, H. J. C.; Fraaije, J. G. E. M. *J. Comput. Chem.* **1997**, *18*, 1463−1472.
(22) Miyamoto, S.; Kollman, P. A. *J. Comput. Chem.* **1992**, *13*, 952−962.
(23) Lippert, R. A.; Bowers, K. J.; Dror, R. O.; Eastwood, M. P.; Gregersen, B. A.; Klepeis, J. L.; Kolossvary, I., *J. Chem. Phys.* **2007**, *126*, 046101.
(24) Ryckaert, J.-P.; Ciccotti, G. *Mol. Phys.* **1986**, *58*, 1125−1136.
(25) Junghans, C.; Prapotnik, M.; Kremer, K. *Soft Matter* **2008**, *4*, 156−161.
(26) Hess, B.; Kutzner, C.; van der Spoel, D.; Lindahl, E. *J. Chem. Theory Comput.* **2008**, *4*, 435−447.
(27) Marrink, S. J.; Risselada, H. J.; Yefimov, S.; Tieleman, D. P.; de Vries, A. H. *J. Phys. Chem. B* **2007**, *111*, 7812−7824.
(28) Berendsen, H. J. C.; Grigera, J. R.; Straatsma, T. P. *J. Phys. Chem.* **1987**, *91*, 6269−6271.
(29) van der Spoel, D.; Lindahl, E.; Hess, B.; van Buuren, A. R.; Apol, E.; Meulenhoff, P. J.; Tieleman, D. P.; Sijbers, A. L. T. M.; Feenstra, K. A.; van Drunen, R.; Berendsen, H. J. C. *Gromacs User Manual Version 4.0*; University of Groningen: Groningen, The Netherlands, 2005. www.gromacs.org (accessed May 2012).
(30) Malevanets, A; Kapral, R. *J. Chem. Phys.* **1999**, *110*, 8605−8613.
(31) Kapral, R. *Adv. Chem. Phys.* **2008**, *140*, 89−146.